Article ID: 1006-8775(2018) 01-0102-09

PREDICTION AND UNCERTAINTY OF CLIMATE CHANGE IN CHINA DURING 21ST CENTURY UNDER RCPS

LIANG Yu-lian (梁玉莲)[1, 2], YAN Xiao-dong (延晓冬)[3], HUANG Li (黄 莉)[1], LU Hong (陆 虹)[4], JIN Shao-fei (靳少非)[5]

(1. Nanning Meteorological Service, Nanning 530028 China; 2. College of Geographical Science and Planning, Guangxi teachers Education University, Nanning 530001 China; 3. State Key Laboratory of Earth Surface Processes and Resource Ecology (ESPRE), Beijing Normal University, Beijing 100875 China; 4. Guangxi Climate Center, Nanning 530022 China; 5. Department of Geography, Ocean College, Minjiang University, Fuzhou 350108 China)

Abstract: Based on integrated simulations of 26 global climate models provided by the Coupled Model Intercomparison Project (CMIP), this study predicts changes in temperature and precipitation across China in the 21st century under different representative concentration pathways (RCPs), and analyzes uncertainties of the predictions using Taylor diagrams. Results show that increases of average annual temperature in China using three RCPs (RCP2.6, RCP4.5, RCP8.5) are 1.87 ℃, 2.88 ℃ and 5.51 ℃, respectively. Increases in average annual precipitation are 0.124, 0.214, and 0.323 mm/day, respectively. The increased temperature and precipitation in the 21st century are mainly contributed by the Tibetan Plateau and Northeast China. Uncertainty analysis shows that most CMIP5 models could predict temperature well, but had a relatively large deviation in predicting precipitation in China in the 21st century. Deviation analysis shows that more than 80% of the area of China had stronger signals than noise for temperature prediction; however, the area proportion that had meaningful signals for precipitation prediction was less than 20%. Thus, the multi-model ensemble was more reliable in predicting temperature than precipitation because of large uncertainties of precipitation.

Key words: CMIP5; RCPs; climate change; model ensemble; prediction; uncertainty; Taylor diagram

CLC number: P435 **Document code:** A

doi: 10.16555/j.1006-8775.2018.01.010

1 INTRODUCTION

Global climate models (GCMs) have an important role in forecasting the future climate in certain preset scenarios. The Coupled Model Intercomparison Project (CMIP), organized by the World Climate Research Program, provides the opportunity for evaluating climate change prediction and attribution analysis using the most current advanced GCMs [1-4]. Based on scenarios designed in the Intergovernmental Panel on Climate Change Fourth Assessment Report (IPCC-AR4), the fifth CMIP (CMIP5), as compared with previous CMIPs[6], improved on ocean-land-atmosphere interaction of the main chemical elements and biophysical processes. CMIP5 also introduced new Representative Concentration Pathways (RCPs) as scenarios of future climate [7]. The RCPs consider the impacts of assumed emissions of greenhouse gases and aerosols, as affected by climate policy. In addition, the application of CMIP5 has been extended from model evaluation to the prediction of future climate [10-14]. The most evaluated indexes are temperature and precipitation in the monsoon region of China [15]. However, most studies were usually based on a single RCP and focused on the normal climate state. Regional differences and seasonal variations, including prediction uncertainties, were little discussed.

Analyzing uncertainties among GCMs can not only evaluate the prediction abilities of models for specific regions but also determine powers of prediction for a single model. The Taylor diagram [16] is a mainstream method to describe model differences. In short, this diagram can combine standard deviation (SD), root mean square error (RMSE), and correlation coefficient (CC), which can be used as predictors to analyze uncertainties of model evaluation [16]. For uncertainty analysis of multi-models, research in the field of climate change has often focused on RMSE [9, 18-20]. For example, based on RMSE, Hu and Ren[14] described the prediction

Received 2017-06-08; **Revised** 2017-12-28; **Accepted** 2018-02-15

Foundation item: Science and Technology Program of Nanning, Guangxi, China (20153257); Major Science and Technology Program of Guangxi, China (GKAB16380267); National Natural Science Foundation of Guangxi (2014GXNSFBA118094, 2015GXNSFAA139243); National Natural Science Foundation of China (41565005); Guangxi Refined Forecast Service Innovation Team

Biography: LIANG Yu-lian, engineer, Ph.D., primarily researching climate change and eco-agriculture.

Corresponding author: JIN Shao-fei, e-mail: shaofei.jin@gmail.com

uncertainty of low temperature events in China; and Li and Zhou [18] discussed the prediction uncertainty of temperature and precipitation in the country under the A1B scenario.

In the present study, based on 26 model outputs of CMIP5, we predicted changes in temperature and precipitation in the 21st century under three RCP scenarios, i.e., RCP2.6, RCP4.5 and RCP8.5. We focused on spatiotemporal responses under those RCPs. We also addressed the deviation of multi-models using the Taylor diagram to ascertain differences and reliabilities of these models in predicting climate change in China. Results of the study can be used to provide climate background data for climate resource and meteorological disaster research in the country in the 21st century, and can also be used as a more accurate source for nesting regional climate models toward higher-resolution results for regional climate[21-23].

2 DATA AND METHODOLOGY

2.1 *Data sources*

The CMIP5 projection data, including monthly precipitation and surface air temperature in RCP2.6, RCP4.5 and RCP8.5, were extracted from outputs of 26 CMIP5 models (https://pcmdi.llnl.gov/projects/esgf-llnl/). Table 1 gives a brief introduction to the CMIP5 models used. Data were rearranged in the ranges 15°−55°N and 70°−140°E, and then interpolated to 1° × 1° from 2011 to 2100 to match observation data. Chinese monthly observed meteorological data from 1986 to 2005 (from the surface temperature/precipitation 1°×1° grid dataset V1.0, provided by the National Meteorological Information Center of the China Meteorological Administration, http://data.cma.cn/) were used as rectification data of CMIP5.

Table 1. Introduction to 26 climate models.

No. of models	Name	Country or Region	Resolution (Row × Column)
1	ACCESS1.0	Australia	145 × 192
2	BCC-CSM1-1	China	64 × 128
3	BNU-ESM	China	64 × 128
4	CANESM2	Canada	64 × 128
5*	CCSM4	USA	192 × 288
6	CESM1-CAM5	USA	192 × 288
7	CMCC-CM	Italy	240 × 480
8	CNRM-CM5	France	128 × 256
9	CSIRO-MK360	Australia	96 × 192
10	EC-EARTH	ECMWF	160 × 320
11	FGOALS-G2	China	60 × 128
12	FIO-ESM	China	64 × 128
13	GFDL-CM3	USA	90 × 144
14	GFDL-ESM2G	USA	90 × 144
15	GISS-E2-H	USA	90 × 144
16	GISS-E2-R	USA	901 × 44
17	HADGEM2-ES	England	192 × 145
18	INM-CM4	Russia	120 × 180
19	IPSL-CM5A-MR	France	143 × 144
20	MIROC5	Japan	128 × 256
21	MIROC-ESM	Japan	64 × 128
22	MIROC-ESM-CHEM	Japan	64 × 128
23	MPI-ESM-LR	Germany	96 × 192
24	MPI-ESM-MR	Germany	96 × 192
25	MRI-CGCM3	Japan	160 × 320
26	NORESM1-M	Norway	96 × 144

2.2 *Data analysis*

The Taylor diagram was used to display the temperature and precipitation predictions of models. This diagram can reflect the degree of discreteness and divergence between a single model and model ensemble using SD, and show their correlation using the CC. Calculation details of the Taylor diagram are in Taylor [16].

The signal (SN) of outputs, which is the ratio of departure (DN) to divergence (DS), was used to measure the effectiveness and credibility of the multi-model ensemble (MME) [18]:

$$SN=\frac{DN}{DS} \quad (1)$$

An effective signal is considered for SN > 1, which indicates that the credibility of results is greater than the noise signal, and vice versa. When DS > DN, there is substantial noise in model results, which must be reduced before the model is used for describing future climate change. Spatial simulation ability differences in

the MME can be reflected by differences among grids. In our study aimed at determining change in China over the 21st century, to estimate DN, we chose the average DN of each cell from 2011 to 2100. For historical reference, we selected the average value from 1986 to 2005. DS was expressed as

$$DS=\sqrt{\frac{1}{N}\sum_{i-0}^{i=N}(Y_i-\overline{Y})^2} \quad (2)$$

where N is the number of models, Y_i is the average value in the estimation period of model i, and $\overline{Y}$ is average value from the MME.

3 RESULTS

3.1 *Temperature variation in China in 21st century projected by multi-model ensemble*

Table 2 lists linear trends of annual average and seasonal average temperatures from the MME (MAM: March, April, May; JJA: June, July, August; SON: September, October, November; DJF: winter: December, January, February) during 2011 –2100. Linear trends of annual average temperature under RCP2.6, RCP4.5, and RCP8.5 are 0.059 ℃ /10yr, 0.229 ℃ /10yr, and 0.590 ℃ /10yr, respectively. The trend under RCP8.5 is ten times that under RCP2.6. The largest growth in temperature was found in DJF under RCP2.6, whereas it was in JJA under RCP4.5 and RCP8.5. These results concur with warming over the 20th century [24]. SON had a faster warming trend than MAM.

Table 2. Linear trend and correlation coefficients of annual and seasonal average temperatures during 2011-2100.

RCPs	linear trend (℃/10yr)					correlation coefficient (R)				
	MAM	JJA	SON	DJF	Annual	MAM	JJA	SON	DJF	Annual
RCP2.6	0.055	0.062	0.059	0.058	0.059	0.60**	0.70**	0.65**	0.55*	0.66**
RCP4.5	0.219	0.220	0.229	0.243	0.229	0.96**	0.98**	0.97**	0.95**	0.97**
RCP8.5	0.567	0.565	0.595	0.636	0.590	0.99**	0.99**	0.99**	0.99**	0.99**

The CCs of regression for RCP4.5 and RCP8.5 are 0.95 and 0.98, respectively. The coefficient for RCP2.6 is 0.6–0.7. All linear regressions passed the significance test with α=0.05, except for DJF under RCP2.6. This illustrates that in the 21st century, average temperature in China under the three RCP scenarios will have a significant increase.

To depict the spatial distribution of temperature change over China in various periods of the 21st century, Fig.1 shows the distribution of annual average temperature anomalies in the country during the early 21st century (2016–2035), middle of the century (2046–2065) and end of the century (2081–2100) relative to the annual average temperature of 1986–2005. Results show that annual average temperatures in China will increase over the 21st century, under all three RCPs. In the early part of the century, warming magnitudes have the following orders: RCP8.5 > RCP2.6 > RCP4.5, and RCP8.5 > RCP4.5 > RCP2.6 in both the middle and end of the century.

The same spatial distributions but different temperature anomalies were found among the three RCPs.

At the end of 21st century, amplitudes of annual average temperature change in China were –0.40 to 4.80 ℃, 1.53 to 5.34 ℃, and 3.26 to 8.56 ℃ under RCP2.6, RCP4.5 and RCP 8.5, respectively. Trends in annual average temperature increased for all China, except for limited regions under RCP2.6. The regions of greatest warming under all three RCPs were the Tibetan Plateau and southern and eastern parts of Xinjiang. Regions of least warming were Inner Mongolia and Northeast China. These projected trends of RCPs roughly agree with warming during the 20th century[25, 26] and with the predictions of MMEs of CMIP3 in AR4[27].

3.2 *Precipitation variation in China over 21st century*

Table 3 shows projected annual and seasonal precipitation anomalies and anomaly percentages for China in the 21st century. Results show that the country will become wetter during that century under all three RCPs. In the early part of the century, precipitation under RCP2.6 and RCP 4.5 increases more than in RCP8.5. During the middle and end of the century, increment magnitudes of precipitation follow order RCP8.5 > RCP4.5 > RCP2.6. However, rates of increase in annual precipitation vary by RCP. Under RCP2.6, an increase in precipitation was found for the early 21st century, and a stable trend at the end of the century (annual precipitation increment is +0.066 mm/day in the early 21st century, +0.059 mm/day in mid-century, and –0.001 mm/day at the end of the century, compared with the period of 1986–2005. Average annual precipitation in China at the end of the 21st century is in line with that in the middle century, but still high (+0.124 mm/day) compared with 1986–2005. Under RCP4.5, compared with previous periods, the annual precipitation increment is +0.067 mm/day in the early 21st century, +0.88 mm/day in mid-century, and +0.059 mm/day at the end of the century. Under RCP8.5, compared with previous periods, the annual precipitation increment is +0.055 mm/day in the early 21st century, +0.129 mm/day in mid-century, and +0.

139 mm/day at the end of the century. All seasonal precipitation is projected to increase, except for DJF of the early 21st century projected under RCP8.5. The increased amplitude of precipitation in JJA is ten times that in DJF.

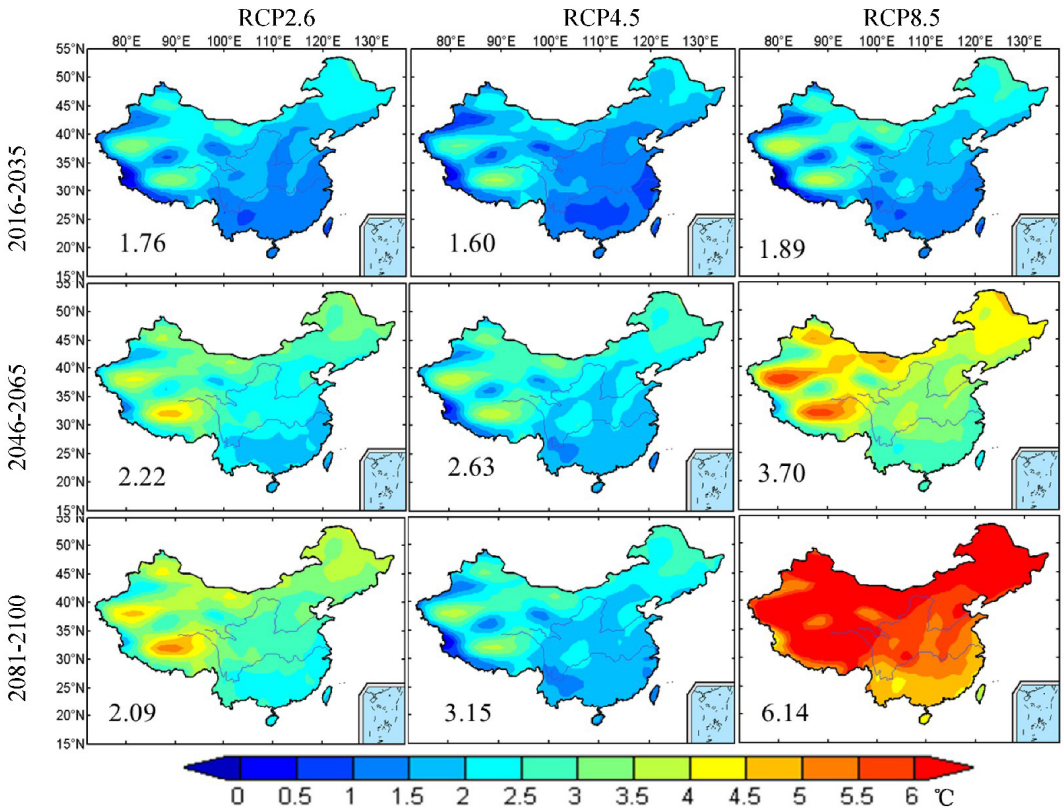

Figure 1. Annual average temperature anomalies during 2016–2035, 2046–2065 and 2081–2100 relative to climatology of 1986–2005. Values at bottom left of each panel shows mean temperature anomaly in China.

Table 3. Linear trend and correlation coefficients of annual and seasonal average temperatures during 2011-2100.

Periods	RCPs	Precipitation anomalies (mm/day)			Precipitation anomaly percentage (%)		
		JJA	DJF	Annual	JJA	DJF	Year
2016	RCP2.6	0.206	0.001	0.066	3.72	0.27	2.71
|	RCP4.5	0.212	0.012	0.067	3.15	1.37	1.59
2035	RCP8.5	0.232	−0.039	0.055	3.97	−4.57	1.04
2046	RCP2.6	0.308	0.011	0.125	5.67	2.24	4.16
|	RCP4.5	0.374	0.052	0.155	6.28	3.78	4.94
2065	RCP8.5	0.471	0.016	0.184	8.21	2.63	6.19
2081	RCP2.6	0.311	0.028	0.124	5.64	2.71	4.04
|	RCP4.5	0.477	0.047	0.214	8.51	6.66	7.33
2100	RCP8.5	0.694	0.066	0.323	12.86	10.88	12.34

Figure 2 shows spatial distributions of annual and seasonal precipitation (JJA and DJF) anomalies in China for 2081–2100, relative to the climatology of 1986–2005. It indicates similar growth in precipitation distributions under the three RCPs, but with different anomalies. The largest increment of annual and summer precipitation is in the southeastern part of the Qinghai-Tibet Plateau, southern part of the Yangtze River, and Northeast China. An increment of annual precipitation >0.30 mm/day under RCP2.6 is found in western Yunnan and most parts of southern China, such as Guangxi and Guangdong. Under RCP4.5, areas with increment of annual precipitation >0.30 mm/day expanded to the southern part of the Qinghai-Tibet Plateau and south of the Yangtze River. Under RCP8.5, in addition to the aforementioned areas, areas with

increase of precipitation >0.30 mm/day embrace most of northern China. The average increment of precipitation in the entire country is also >0.30 mm/day, compared to the present period. The most obvious increase in winter precipitation is in the middle and lower reaches of the Yangtze River. These spatial distributions have substantial consistency with Li [18], who projected the distribution of precipitation in the 21st century under the A1B scenario, based on the data of CMIP3.

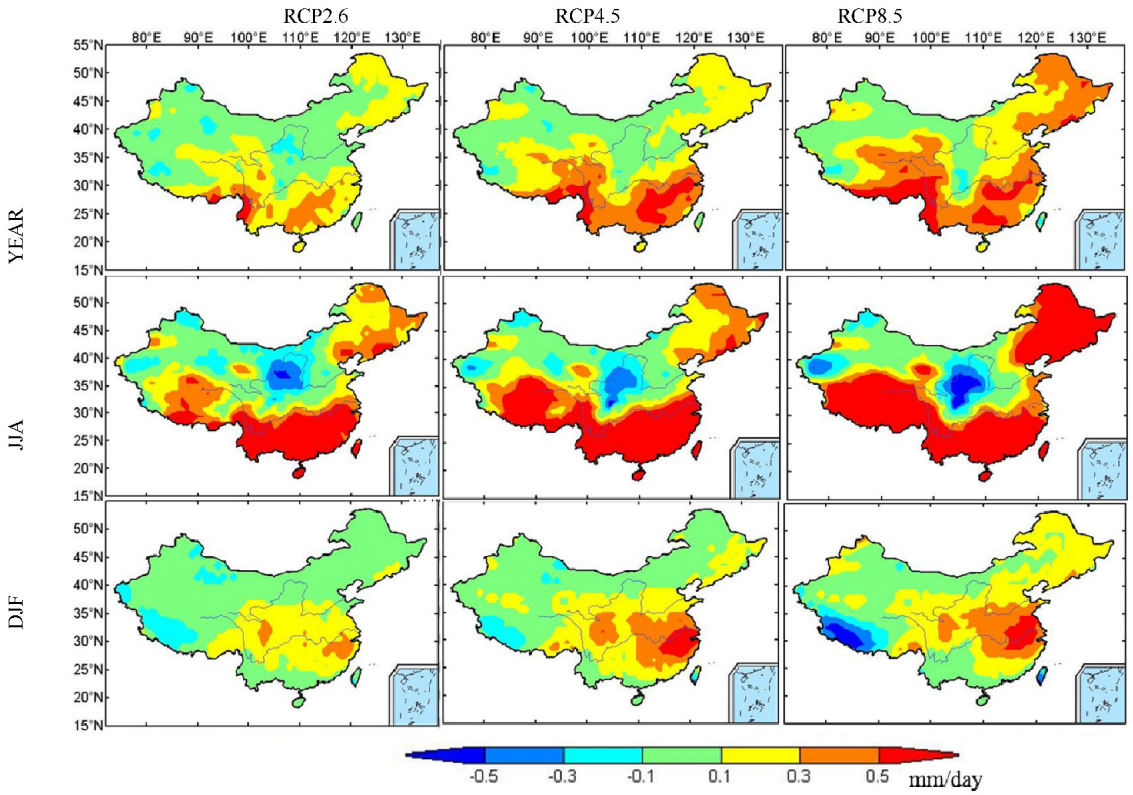

Figure 2. Annual/JJA/DJF precipitation anomalies during 2081–2100 projected by MME.

For areas of decreased precipitation, annual precipitation is not identical to that of winter or summer. For annual precipitation, areas with variation < –0.1 mm/day is only irregularly distributed, in the central region and western part of northwestern China, under all RCPs. For summer precipitation, there was a decreasing trend in central China, especially in the Shaanxi –Gansu –Ningxia region, where summer precipitation decline is more than 0.5 mm/day. These results are similar to the conclusion in IPCC-AR5[12, 28].

4 ANALYSIS OF UNCERTAINTY

4.1 *Uncertainty of single models*

Taking the RCP4.5 scenario as representative, Fig.3 shows the Taylor diagram of annual temperature and precipitation in 2011–2100 projected by 26 models, as compared with MME. Results show that uncertainty of the temperature projection is obviously smaller than that of the precipitation projection. Temperature deviation in the diagram (Fig.3a) shows SDs of single models compared with MME between 0.75 and 1.5; their CC is between 0.8 and 0.95, all of which pass the significance test with α=0.05. SDs of the BNU-ESM, CNRM-CM5 and MPI-ESM-MR are closest to the MME, with CC ~0.9. SDs of the GFDL-CM3, HADGEM2-ES, MIROC-ESM and MIROC-ESM-CHEM models are > 1.5, but with large CCs (~0.95).

Compared to temperature, predicted precipitation was more discrete, and SDs of single models compared to the MME are between 1.0 and 2.5. The fluctuation of single models for precipitation projection is much greater than the MME. CC differences ranged from 0.08 to 0.8. Twenty-five models passed the significance test, except FIO-ESM. That model had the greatest divergence (SD=1.72 and CC<0.1). SDs of the EC-EARTH, FGOALS-G2, GFDL-ESM2G models, as compared with the MME, are smaller, but their CCs did not reach 0.5.

4.2 *Uncertainty of MME*

The spatial distribution of DS of temperature shows that regions with large temperature variation are in western China, especially the western parts of Xinjiang and Tibet (Fig.4). This indicates that projection uncertainty of temperature is greater in those areas than others, e.g., the entire central plains and southern regions of the country. Similar patterns are drawn from uncertainty studies of CMIP3 models[27].

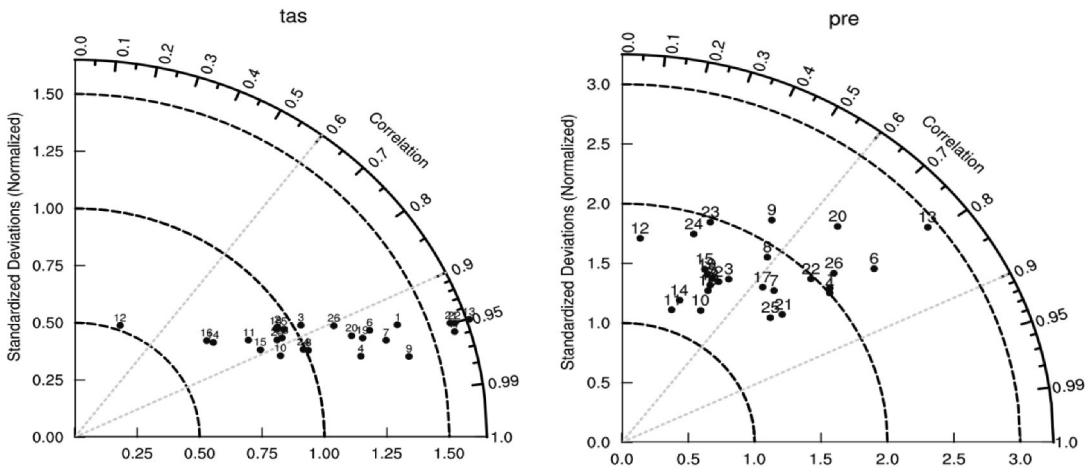

Figure 3. Taylor diagram of annual mean surface air temperature (left) and annual average precipitation (right) for China in 21st century as predicted by 26 CMIP5 models, compared with MME under RCP4.5.

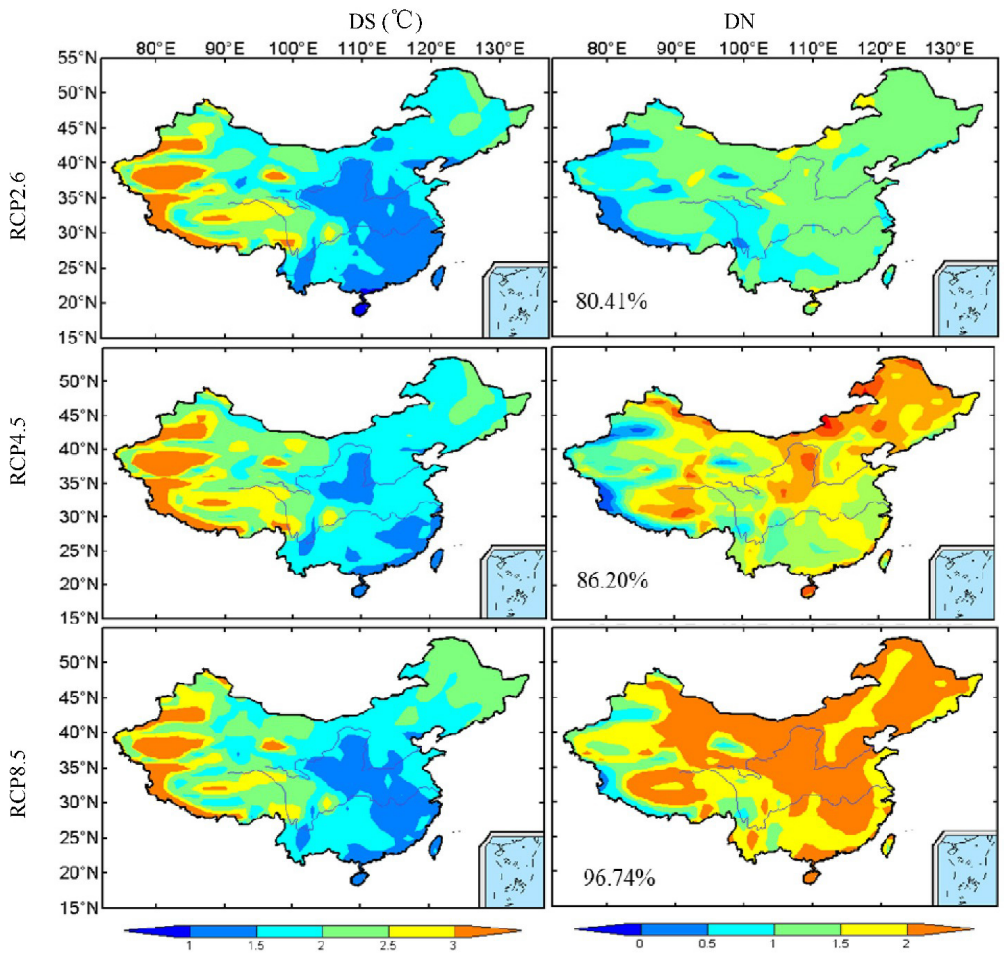

Figure 4. Annual average temperature deviation (left panels) and signal of MME (right panels). Values at bottom left of right panels is area ratio of meaningful signal; the same in Fig.5).

The spatial distribution of DN is similar to that of DS. Area ratios for DN > 1 are 80.41%, 86.20% and 96.74% under RCP2.6, RCP4.5 and RCP8.5, respectively. This illustrates that the temperatures projected by the MME are meaningful signals in most areas of the country, except Xinjiang.

The DS of precipitation under the three RCPs shows similar spatial distributions. DS ranged from 0 to 2 mm/day (Fig.5). The effect sizes of DS are constrained by the basic distribution of the precipitation anomalies. Area ratios for DN>1 are < 20% of the total area of China under the three RCPs. This reveals that

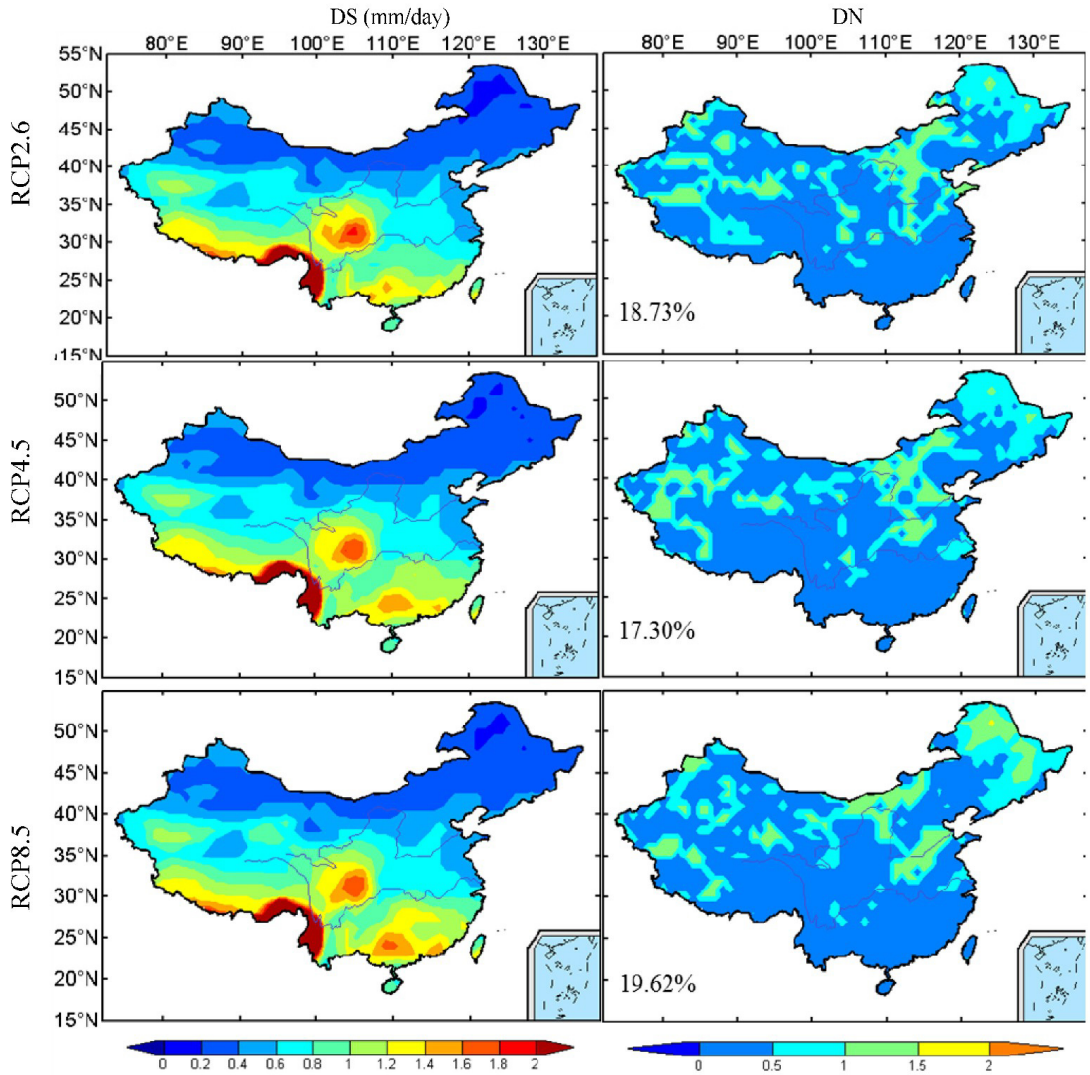

Figure 5. Annual average precipitation deviation (left panels) and signal (right panels) of MME.

the results projected by the MME in most areas of the country have weak credibility with the 1°×1° resolution. Thus, using these projected data directly in other fields of climate change should be done with caution.

5 CONCLUSIONS

(1) Projections of the MME of CMIP5 models show a warming and wetting China over the 21st century under each RCP.

(2) The Taylor diagrams show that SDs of annual temperature of 26 single models compared to MME are between 0.75 and 1.5; their CC is between 0.8 and 0.95 under the RCP4.5 scenario. The SD distribution of annual precipitation is more discrete and the CC is between 0.3 and 0.8. Differences and uncertainties of CMIP5 models for precipitation projection are much larger than those of temperature.

(3) Divergence analysis of the MME shows that the signal in the projection result of temperature is larger than the noise.

6 DISCUSSION

Under the RCP2.6 scenario, both temperature and precipitation will remain stable in the mid-21st century. This highlights the effects of emission concentration control policy on climate changes [7]. Under RCP4.5 and RCP8.5, temperature continues to rise over the 21st century. Amplitudes and rates of temperature change are directly associated with radiation forcing in the RCPs[7], i.e., the greater the forcing, the greater the increase in temperature. The projection results of temperature in the low, medium and high emission scenarios in IPCC-AR5 have good correspondence with the three emission scenarios in IPCC-AR4 [27]. By the end of the 21st century, the amplitude of temperature increase in China under different scenarios of IPCC-AR5 and IPCC- AR4 has the order RCP2.6 < B1, RCP4.5 < A1B, RCP8.5 > A2, with the greatest increase over the Tibetan Plateau and Northeast China. Change in precipitation is not consistent with results from the IPC-AR5 and

IPCC-AR4 scenarios. At the end of the 21st century, the increase of precipitation in China under the three RCPs ranges from 4.04% to 12.34%, with greater increases for higher-concentration pathways. Increases of the three scenarios in IPCC-AR4 are from 7.21% to 9.83% and the largest is under A1B, which does not have the greatest emission [19]. The difference of precipitation projection under the new RCP scenarios is greater than in older scenarios.

GCMs have been a credible approach to projecting temperature and researching future climate change impacts. However, using the precipitation projection data directly in other fields of climate change should be done with caution. Influenced by accuracy of the GCMs and other factors (e.g., mode and model selection, model resolution, and data interpolation methods), projection results vary in quantity or even in trends within areas of light precipitation. The projection results can only give possible future trends of precipitation to a certain degree. Therefore, to obtain more accurate and reliable climate prediction data, it is necessary to rely on a more complex and accurate global land–sea–air coupled model, incorporate more realistic economic and social scenarios, and use more detailed downscaling approaches. These tasks are the basis for future research in other fields of climate change impact assessment.

Acknowledgement: We are grateful to the Program for Climate Model Diagnosis and Intercomparison (PMCDI, http://cmip-pcmdi.llnl.gov/cmip5/) for providing data of CMIP5 models.

REFERENCES:

[1] KHARIN V V, ZWIERS F W. Climate predictions with multimodel ensembles [J]. J Climate, 2002, 15 (7): 793-799.

[2] JIANG Da-bang, WANG Hui-jun, LANG Xian-mei. Multimodel ensemble prediction climate change trend of China under SRES A2 scenario [J]. Chin J Geophys, 2004, 47(5): 777-785.

[3] MIN S, HENSE A A. Bayesian approach to climate model evaluation and multi-model averaging with an application to global mean surface temperatures from IPCC AR4 coupled climate models [J]. Geophys Res Lett, 2006, 33 (8): L8708.

[4] ZHAO Zong-ci, LUO Yong, JIANG Ying, et al. Projections of surface air temperature change in China for the next two decades [J]. J Meteor & Environ, 2008, 24 (5): 1-5.

[5] ANNAN J D, HARGREAVES J C. Reliability of the CMIP3 ensemble [J]. Geophy Res Lett, 2010, 37 (2): L02703.

[6] TAYLOR K E, STOUFFER R J, MEEHL G A. An overview of CMIPS and the experiment design [J]. Bull Amer Meteor Soc, 2012, 93(4): 485-498.

[7] CHEN Min-peng, LIN Er-da. Global greenhouse gas emission mitigation under representative concentration pathways scenarios and challenges to China [J]. Adv Clim Change Res., 2010, 6(6): 436-442.

[8] JIANG Yan-min, WU Hao-min. Simulation capabilities of 20 CMIP5 models for annual mean air temperatures in Central Asia [J]. Adv Clim Change Res, 2013, 9 (2): 110-116.

[9] CHEN Xiao-chen, XU Ying, XU Cong-hai, et al. Assessment of precipitation simulations in China by CMIP5 multi-models [J]. Adv Clim Change Res, 2014, 10 (3): 217-225.

[10] KHARIN V V, ZWIERS F W, ZHANG X, et al. Changes in temperature and precipitation extremes in the CMIP5 ensemble [J]. Clim Change, 2013, 119(2): 345-357.

[11] WU Hao-min, HUANG An-ning, HE Qing, et al. Projection of the spatial and temporal variation characteristics of precipitation over Central Asia of 10 CMIP5 models in the next 50 years [J]. Arid Land Geography, 2013, 36(4): 670-679.

[12] XIN Xiao-ge, CHENG Yan-jie, WANG Fang, et al., Asymmetry of surface climate change under RCP2.6 projections from the CMIP5 models [J]. Adv Atmos Sci, 2013, 30(3): 769-805.

[13] LIU Yong-he, FENG Jin-ming, MA Zhu-guo. An analysis of historical and future temperature fluctuations over China based on CMIP5 simulations [J]. Adv Atmos Sci, 2014, 31(3): 457-467.

[14] HU Hao-lin, REN Fu-min. Simulation and projection for China's regional low temperature events with CMIP5 multi-model ensembles [J]. Adv Clim Change Res, 2016, 12(5): 396-406.

[15] LI Rui-qing, LV Shi-hua, HAN Bo. Simulations of Asian-Australian monsoon circulation and variability by 10 CMIP5 models [J]. J Trop Meteor, 2013, 29 (5): 749-758.

[16] TAYLOR K E. Summarizing multiple aspects of model performance in single diagram [J]. J Geophys Res, 2001, 106(D7): 7183-7192.

[17] GUO Yan, DONG Wen-jie, REN Fu-min, et al. Assessment of CMIP5 simulations for China annual average surface temperature and its comparison with CMIP3 simulations [J]. Adv Clim Change Res, 2013, 9 (3): 181-186.

[18] LI Bo, ZHOU Tian-jun. Projected climate change over China Under SRES A1B scenario: Multi-model ensemble and uncertainties [J]. Adv Clim Change Res, 2010, 6(4): 270-276.

[19] HUA Wen-jian, CHEN Hai-shan, SUN Shan-lei. Uncertainty in land surface temperature simulation over China by CMIP3/CMIP5 climate models [J]. Theor Appl Climatol, 2014, 117(3-4): 463-474.

[20] GU Wen, CHEN Bao-de, YANG Yu-hua, et al. Simulation evaluation and uncertainty analysis for climate change projections in East China made by IPCC-AR4 models [J]. Prog Geogr, 2010, 29(7): 270-276.

[21] LI Xin-zhou, LIU Xiao-dong. Numerical simulations of extreme precipitation in eastern China under A1B scenario [J]. J Trop Meteor, 2012, 27(3): 379-391.

[22] DU Yao-dong, YANG Hong-long, LIU Wei-qin. Future change of precipitation extremes over the pearl river from regional climate models [J]. J Trop Meteor, 2014, 30(3): 495-502.

[23] YANG Hong-long, WANG Bing-kun, DU Yao-dong, et al. Projected change in mean climate in the pearl river basin under the RCPs scenarios [J]. J Trop Meteor, 2014,

30(3): 503-510.
[24] TANG Guo-li, REN Guo-yu. Reanalysis of surface air temperature change of the last 100 years over China [J]. Clim Environ Res, 2005, 10(4): 791-798.
[25] ZUO Hong-chao, LV Shi-hua, HU Yin-qiao. Variations trend of yearly mean air temperature and precipitation in China in the last 50 Years [J]. Plateau Meteor, 2005, 23 (2): 238-244.
[26] IPCC. Climate Change 2007: The Physical Science Basis. Working Group I Contribution to the Fourth Assessment Report of the Intergovernmental Panel on Climate Change [M]. Cambridge: Cambridge University Press, 2011: 21-253.
[27] JIANG Zhi-hong, ZHANG Xia, WANG Ji. Projection of climate change in China in the 21st century by IPCC-AR4 models [J]. Geogr Res, 2008,27(4): 787-799.
[28] IPCC. Climate Change 2013: The Physical Science Basis: Working Group I Contribution to the Fifth Assessment Report of the Intergovernmental Panel on Climate Change [M]. Cambridge: Cambridge University Press, Cambridge University Press, 2014: 83,145.

Citation: LIANG Yu-lian, YAN Xiao-dong, HUANG Li, et al. Prediction and uncertainty of climate change in China during 21st century under RCPs [J]. J Trop Meteor, 2018, 24(1): 102-110.